Amide Backbone and Water-Related H/D Isotope Effects on the Dynamics of a Protein Folding Reaction

Martin J. Parker* and Anthony R. Clarke

Department of Biochemistry, University of Bristol, School of Medical Sciences, University Walk, Bristol, BS8 1TD, U.K.

Received November 27, 1996; Revised Manuscript Received March 13, 1997[⊗]

ABSTRACT: The denaturant-dependent relaxation kinetics of folding and unfolding of an isolated *all-β* domain of rat CD2 have been measured at 25 °C in four isotopic conditions: with a protonated (amide) backbone in H_2O and in D_2O and with a deuterated backbone in H_2O and in D_2O. The data show that this structure, which contains no disulfide bonds, folds through a rapidly formed intermediate (pathway U-I-F) and that all free energy changes between states are insensitive to isotopic substitution of the amide groups required for intrachain hydrogen bonding. However, the folding reaction is significantly influenced by the nature of the bulk solvent. In D_2O, the stability of each state in the folding pathway, relative to the unfolded molecule, is enhanced to a degree which is proportional to its *m* value, a measure of the exposure of nonpolar protein groups to the solvent. Together these observations suggest that, at this temperature, the solvent isotope effect arises from enhanced hydrophobic interactions which, in turn, results from an increased strength of the solvent−solvent hydrogen bond in D_2O. Apart from emphasizing the role of bonds between solvent molecules in protein folding, the results also have practical implications for amide H/D exchange studies. While the replacement of amide protons by deuterons will not affect the protein's stability during exchange experiments, it is important to account for the isotopic influence of the solvent in which the exchange reaction is performed.

The modest stability of protein molecules, under physiological conditions, results from a fine balance between large stabilizing and destabilizing forces (Creighton, 1991; Dill, 1990). The reduction in conformational entropy upon folding is outweighed, in principle, by a combination of intramolecular hydrogen bonding and the hydrophobic interaction, but their relative contribution remains a contentious issue. While some contest that the hydrophobic interaction is the dominant force in protein folding (Dill, 1990; Honig & Yang, 1995), others maintain that backbone hydrogen bonding makes a comparable contribution to the stability of the folded state (Makhatadze & Privalov, 1994; Pace *et al*., 1996).

The influence of H_2O and D_2O on protein stability is linked to these two effects in the following way. The isotopic substitution of hydrogen by deuterium has been shown to affect the strength of (a) solvent−solvent, (b) solute−solute, and (c) solute−solvent hydrogen bonds [for examples see Benjamin and Benson (1962), Creswell and Allred (1962), Kresheck *et al*. (1965), and Scheiner and Cuma (1996)]. Hence, the documented changes in stability and folding rates of proteins in D_2O (Hermans & Scheraga, 1959; Makhatadze *et al*., 1995; Itzhaki & Evans, 1996) could result from any combination of these effects. That is, changes in bond strength between water molecules will influence the hydrophobic interaction, while changes in amide−carbonyl, amide−water, or carbonyl−water bond strengths will influence the net contribution made by backbone hydrogen bonding.

In the study presented here we attempt to dissect hydrogen/deuterium isotope effects on these different bonds and assess their effect on each state in the folding pathway of a small (98-residue) *all-β* protein, domain 1 of rat CD2 (Driscoll *et al*., 1991). Topologically, this structure belongs to the IgG superfamily but unusually contains no disulfide bridges. To examine these isotope effects, the relaxation rates of folding and unfolding of this isolated domain of CD2 are determined as a function of denaturant concentration in four isotopic regimes; (i) with (backbone) protonated CD2 in H_2O, (ii) with deuterated CD2 in H_2O, (iii) with protonated CD2 in D_2O, and (iv) with deuterated CD2 in D_2O. By using conditions where amide hydrogen exchange is much slower than relaxation rates, we avoid the difficulty of partial exchange over the time course of measurement.

MATERIALS AND METHODS

Experimental Procedures

Source of Protein. Domain 1 of rat CD2 (residues 1−98) was expressed in *Escherichia coli* as a fusion protein with glutathione-*S*-transferase (GST)[1] using the pGEX-2T gene fusion vector (Pharmacia) (Driscoll *et al*., 1991). This gene construct was transformed into *E. coli* HB2151 cells (Pharmacia), a non-amber suppressing strain. The protein purification procedure described here differs from that originally described by Driscoll *et al*. (1991). Cells grown overnight at 37 °C in NZCYM broth containing 0.5 mg mL^{-1} ampicillin (Beecham Research) were diluted 1:10 into fresh

* Author to whom correspondence should be addressed.

[⊗] Abstract published in *Advance ACS Abstracts,* May 1, 1997.

[1] Abbreviations: bis-Tris, bis(2-hydroxyethyl)iminotris(hydroxymethyl)-methane; ^{NH}CD2, protonated CD2; NDCD2, deuterated CD2; D_2O, deuterium oxide; DTT, dithiothreitol; EDTA, ethylenediaminetetraacetic acid; GuHCl, guanidine hydrochloride; GuDCl, GuHCl with the exchangeable protons replaced by deuterons; GST, glutathione-*S*-transferase; IPTG, isopropyl *β*-D-thiogalactoside; NATA, *N*-acetyltryptophanamide; NMR, nuclear magnetic resonance; PMSF, phenylmethylsulfonyl fluoride; SDS−PAGE, sodium dodecyl sulfate polyacrylamide gel electrophoresis; Tris·HCl, tris(hydroxymethyl)-methylamine hydrochloride.

S0006-2960(96)02928-5 CCC: $14.00

media and grown at 37 °C to mid-log phase. Isopropyl β-D-thiogalactoside (IPTG; Sigma) was then added to 1 mM, and the cells were grown for an additional 2−3 h. Cells were harvested by centrifugation and resuspended in 30 vol of ice-cold resuspension buffer [TBS, pH 7.4, (Sambrook *et al*., 1989) and 5 mM ethylenediaminetetraacetic acid (EDTA; Sigma)]. 100 μg mL^{-1} hen egg white lysozyme (Sigma) and 0.2 mM phenylmethylsulfonyl fluoride (PMSF; Sigma) were then added, and the cells were incubated on ice for 30−45 min. Dithiothreitol (DTT; Sigma) was then added to 5 mM. The cells were subjected to mild sonication for 20 s on ice, and 0.2 mM PMSF was added immediately. Triton X-100 (Sigma) was then added to 1.0%, the suspension mixed thoroughly and any insoluble material removed by centrifugation (10 000*g* for 20 min). The supernatant was then loaded onto a glutathione Sepharose 4B (Sigma) column, equilibrated in resuspension buffer, 5 mM DTT, and 1.0% Triton X-100 at 4 °C. The column was washed with 10 vol of this buffer and the fusion protein eluted with 10 mM reduced glutathione (Sigma) in 50 mM tris(hydroxymethyl)methylamine hydrochloride (Tris·HCl), pH 8.0 (Boehringer Mannheim). Fractions containing >90% pure fusion protein, as assessed by SDS−PAGE, were pooled and dialyzed against 200 vol of 50 mM Tris·HCl, pH 8.0, 150 mM NaCl, and 2.5 mM $CaCl_2$. 6 units mL^{-1} of thrombin (Boehringer Mannheim) was then added, and the solution was left for 3 h at room temperature for the digest to reach completion (as assessed by SDS−PAGE). The protein was then dialyzed against 200 vol of 50 mM bis(2-hydroxyethyl)-iminotris(hydroxymethyl)methane (bis-Tris), pH 5.5 (Sigma), and loaded onto a column containing fast flow S-sepharose (Pharmacia) equilibrated in the same buffer. After GST had been washed through, CD2 was eluted to high purity with 0.5 M NaCl. As CD2 samples purified in this manner contain a small fraction of dimer (Murray *et al*., 1995), the protein was unfolded by the addition of 3 M guanidine hydrochloride (GuHCl; enzyme grade, Sigma) and then refolded by dialyzing twice against 200 vol of 50 mM Tris·HCl, pH 7.0. All of the resultant protein is monomeric, as assessed by native PAGE. Pure CD2 was then concentrated using 3 kDa cutoff Centriplus centrifugal concentrators (Amicon) and then 0.02% sodium azide added before storage at 4 °C.

To produce deuterium-labeled CD2, the protein was dialyzed overnight against D_2O (Sigma), buffered at pH 9−9.5 with 50 mM Tris·HCl. For both equilibrium and kinetic measurements, protonated/deuterated CD2 was dialyzed against 50 mM sodium acetate (Sigma) in H_2O/D_2O at a measured pH (pH_m) of 4.5/4.1.

Protein concentrations were estimated by UV absorption of aromatic residues at 280 nm [ϵ = 5500 M^{-1} cm^{-1} for tryptophan (two residues) and 1100 M^{-1} cm^{-1} for tyrosine (two residues)].

Deuterated Guanidine Hydrochloride (GuDCl). GuHCl was dissolved in D_2O to a concentration of 3 M. The solvent was then removed using a rotary evaporator. This procedure was repeated 6 times until the exchangeable protons were reduced to <1%. Residual solvent was then removed by lyophilization, where the weight of the sample was monitored over time to ensure complete removal of solvent. GuDCl was stored in a desiccator prior to being dissolved in D_2O.

Equilibrium Unfolding Measurements. Consecutive additions of a concentrated stock of GuHCl/GuDCl were made to 2 μM solution of protonated/deuterated CD2 at 25 °C in 50 mM sodium acetate in H_2O/D_2O (pH_m 4.5/4.1) in a quartz cuvette. With each addition, the solution was mixed thoroughly and the reaction allowed to reach equilibrium before the fluorescence intensity was recorded. An excitation wavelength of 285 nm was selected by a single monochromator (slit width 1 nm) from a xenon light source, and the fluorescence intensity at 330 nm was recorded using a single-emission monochromator (slit width 5 nm) in a Spex Fluoromax spectrofluorometer. All data were corrected for dilution.

Measurements of the Kinetics of Folding and Unfolding. Folding reactions were initiated by mixing a 10 μM solution of unfolded, protonated/deuterated CD2, containing 50 mM sodium acetate in H_2O/D_2O, pH_m 4.5/4.1, and 2 M GuHCl/GuDCl, against 10 vol of buffered H_2O/D_2O, containing an appropriate concentration of GuHCl/GuDCl, at 25 °C, in an Applied Photophysics stopped-flow apparatus. An excitation wavelength of 288 nm was selected by a single monochromator (slit width 5 nm) from a mercury−xenon light source, and the fluorescence intensity above 320 nm was recorded using an emission cutoff filter. For the unfolding reactions, a 10 μM solution of folded, protonated/deuterated CD2, containing 50 mM sodium acetate in H_2O/D_2O, pH_m 4.5/4.1, was mixed against 10 vol of buffered H_2O/D_2O, containing an appropriate concentration of GuHCl/GuDCl, at 25 °C, and the reaction recorded as above. For measurements of the dependence of the folding rate on solution viscosity, a 20 μM solution of protonated CD2, containing 3 M GuHCl and 50 mM sodium acetate (pH 4.5), was mixed against 10 vol of 50 mM sodium acetate (pH 4.5) containing 0, 5, 10, and 15% (v/v) glycerol (BDH, AnalaR grade) at 25 °C and the folding rate recorded as above.

Solubility Measurements. Saturated solutions of *N*-acetyltryptophanamide (NATA) (Sigma) were made-up in H_2O/D_2O, containing an appropriate concentration of GuHCl/GuDCl. The solutions were sonicated and then incubated for 48 h at 25 °C with vigorous shaking, to allow complete equilibration. Insoluble material was then removed by centrifugation. The concentration of soluble NATA in each sample was then assessed by measuring the absorbance at 280 nm at 25 °C.

All reaction solutions were maintained at 25 °C using thermostated circulating water baths, and were monitored continuously with a sensitive thermocouple. From this, the fluctuation in temperature was determined to be no more than ±0.1 °C.

Analytical Procedures

Denaturant Activity. For the analysis of equilibrium and kinetic data, guanidine hydrochloride concentration ([GuHCl]) is converted to molar denaturant activity (*D*), according to the relationship

$$D = C_{0.5}[\text{GuHCl}]/(C_{0.5} + [\text{GuHCl}]) \qquad (1)$$

where $C_{0.5}$ is a denaturation constant with the value 7.5 M [see Parker *et al*. (1995) and Results]. For data collected in D_2O, a $C_{0.5}$ value of 9.1 M is used, derived from the solubility data for NATA (see below and Results).

Treatment of Equilibrium Data. Equilibrium fluorescence profiles were fitted using the Grafit programs (Erithracus

Software) to the equation

$$I = \alpha_F I_F + \alpha_U I_U \quad (2)$$

with temporary variables

$$K_{F/U} = K_{F/U(w)} \exp(m_U D)$$

$$\alpha_F = K_{F/U}/(1 + K_{F/U})$$

$$\alpha_U = 1 - \alpha_F$$

where α_F and α_U are the fractional populations of molecules in the folded and unfolded states, respectively; I, I_F, and I_U are the fluorescence intensities (measured, folded, and unfolded), $K_{F/U}$ is the equilibrium constant ([F]/[U]) at a given denaturant activity, $K_{F/U(w)}$ is this equilibrium constant in water, and m_U describes the exponential reduction in $K_{F/U}$ as a function of the denaturant activity; it has units of M^{-1} (Parker *et al*., 1995).

Treatment of Kinetic Data. The transients of fluorescence intensity (I) *versus* time, which are single, first-order processes, in both the folding and unfolding directions, were fitted to the equation $I = I_a(1 - \exp(-kt)) + I_o$ for rising intensities (where I_a is the fluorescence amplitude of the reaction, k is the observed rate constant for the relaxation, and I_o is the initial intensity), and to $I = I_a \exp(-kt) + I_f$ for decreasing intensities (where I_f is the final fluorescence intensity).

Linear free energy profiles [observed rate constant (k_{obs}) *versus* denaturant activity] were fitted to eq 3:

$$k_{obs} = k_{F-I} + k_{I-F}/(1 + 1/K_{I/U}) \quad (3)$$

[see Parker *et al*. (1995) and Results] where k_{I-F} and k_{F-I} are rate constants describing the forward and reverse transitions, respectively, between the folded and intermediate states and $K_{I/U}$ is the equilibrium constant for the rapid interconversion of the intermediate and unfolded states. In the fitting routine the following temporary variables were used:

$$k_{F-I} = k_{F-I(w)} \exp(-m_t D)$$

$$k_{I-F} = k_{I-F(w)} \exp((m_I - m_t)D)$$

$$K_{I/U} = K_{I/U(w)} \exp((m_U - m_I)D)$$

where the subscript w describes the rate and equilibrium constants in water and the m parameters describe the shifts in the stabilities of each state (designated by the subscript) as a function of denaturant activity (D) and have units of M^{-1} (note that these are measured relative to the folded state, F).

Treatment of Solubility Data. The difference in the free energy of solvation (ΔG_s) for NATA between water and a given concentration of GuH/DCl is given by

$$\Delta G_s = -RT \ln(A_{280}/A_{280(w)}) \quad (4)$$

where A_{280} is the absorbance at 280 nm measured in a particular concentration of GuH/DCl and $A_{280(w)}$ is that measured in H_2O/D_2O. Plots of ΔG_s *versus* [GuH/DCl] were fitted to the hyperbolic relationship

$$\Delta G_s = \Delta G_{s,max}[\text{GuH/DCl}]/(C_{0.5} + [\text{GuH/DCl}]) \quad (5)$$

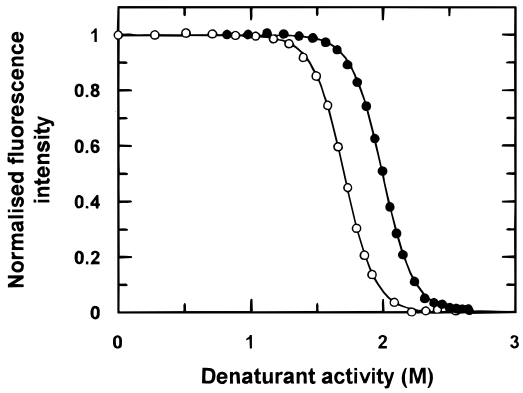

FIGURE 1: Equilibrium unfolding. The fluorescence intensity of CD2, arising from its two tryptophan residues, was measured at increasing concentrations of the denaturant guanidine hydrochloride ([GuHCl]), at 25 ± 0.1 °C (see Experimental Procedures): open circles, protonated CD2 in H_2O (pH_m 4.5); closed circles, deuterated CD2 in D_2O (pH_m 4.1), using deuterated GuHCl (GuDCl). In this plot, [GuHCl] has been converted to denaturant activity, according to eq 1, using values of $C_{0.5}$ of 7.5 M for H_2O and 9.1 M for D_2O (see Results for explanation). Both sets of data represent single structural transitions and have been fitted to eq 2, to yield values of $K_{F/U(w)}$, the equilibrium constant F/U in water, and m_U, which describes the sensitivity of this equilibrium to the denaturant activity. No base line corrections are required when fitting these data. The data have been normalized solely for protein concentration, and both sets of data represent averages of two repeated experiments. Fits to the data are shown as continuous curves, and the calculated values of $K_{F/U(w)}$ and m_U are given in Table 1.

where $\Delta G_{s,max}$ is the maximum change in the free energy of solvation at an infinite concentration of denaturant and $C_{0.5}$ is a denaturation constant with units of M.

All data were fitted using the Grafit analysis software (Erithracus Software, U.K.). When kinetic data were fitted to eq 3, proportional weighting was used so that the fitted values took account of rate constants equally across the whole range.

RESULTS

Folding Pathway of CD2

The fully reversible equilibrium folding profile of CD2 (H_2O, pH 4.5) is shown in Figure 1. This profile represents a single structural transition, i.e., the only species populated in the equilibrated system are the fully folded (F) and unfolded (U) states. As the protein unfolds, the two emission maxima, at 315 and 330 nm, shift to a single maximum at 355 nm and the total fluorescence intensity falls by ~80% (data not shown). The GuHCl concentration has been converted to molar denaturant activity (D) using eq 1 (see below for discussion). The equilibrium data are fitted to eq 2, which describes a single equilibrium process, to yield values of $K_{F/U(w)}$ (the equilibrium constant (F/U) in water) and m_U (a measure of the sensitivity of this equilibrium to the denaturant activity). This latter parameter provides a measure of the difference in the solvation of hydrocarbon between F and U (Shortle *et al*., 1988; Staniforth *et al*., 1993; Parker *et al*., 1995 & 1996; Myers *et al*., 1995; see also Supporting Information). Values of $K_{F/U(w)}$ and m_U for CD2 are given in Table 1.

Fluorescence transients which report the folding and unfolding kinetics of CD2 (H_2O, pH 4.5) are shown in Figure 2a and 2b, respectively, and describe single exponential

Table 1: Folding Parameters for Protonated/Deuterated CD2 in H_2O/D_2O

	^{NH}CD2−H_2O[a]	^{NH}CD2−D_2O[b]	NDCD2−H_2O[a]	NDCD2−D_2O[b]
$k_{I-F(w)}$ (s^{-1})	13.9 ± 0.8	18.9 ± 1.0	13.2 ± 0.6	16.5 ± 0.7
$k_{F-I(w)}$ (s−1)	(1.04 ± 0.18) × 10^{-4}	(3.94 ± 0.97) × 10^{-5}	(9.60 ± 0.24) × 10^{-5}	(3.53 ± 0.46) × 10^{-5}
$K_{I/U(w)}$	19.5 ± 2.0	42.3 ± 7.7	17.7 ± 1.7	49.0 ± 7.2
$\Delta G_{I-U(w)}$ (kcal mol^{-1})	−1.75 ± 0.01	−2.21 ± 0.11	−1.69 ± 0.06	−2.29 ± 0.09
$K_{F/U(w)}$[c]	(2.61 ± 0.86) × 10^6	(2.03 ± 0.88) × 10^7	(2.43 ± 0.40) × 10^6	(2.30 ± 0.74) × 10^7
	[(1.78 ± 0.50) × 10^6]			[(2.58 ± 0.55) × 10^7]
$\Delta G_{F-U(w)}$ (kcal mol^{-1})	−8.71 ± 0.24	−9.92 ± 0.27	−8.67 ± 0.10	−9.99 ± 0.19
	[−8.49 ± 0.17]			[−10.1 ± 0.1]
m_I (M^{-1})	−5.08 ± 0.14	−5.03 ± 0.12	−5.00 ± 0.15	−5.02 ± 0.09
m_t (M^{-1})	−3.19 ± 0.07	−3.26 ± 0.05	−3.24 ± 0.10	−3.24 ± 0.06
m_U (M^{-1})	−8.44 ± 0.10	−8.56 ± 0.09	−8.55 ± 0.08	−8.51 ± 0.09
	[−8.40 ± 0.17]			[−8.57 ± 0.12]

[a] Denaturant activity scale calculated using $C_{0.5}$ = 7.5 M. [b] Denaturant activity scale calculated using $C_{0.5}$ = 9.1 M (see legend to Figure 5). [c] $K_{F/U(w)} = [k_{I-F(w)}/k_{F-I(w)}]K_{I/U(w)}$. The values in brackets of $K_{F/U(w)}$ and m_U for ^{NH}CD2 in H_2O and NDCD2 in D_2O were derived from the equilibrium unfolding profiles in Figure 1, using eq 2. Extracting six independent variables from one data set may result in relatively large fitting uncertainties. However, apart from the high reproducibility of these rate profiles in both H_2O and D_2O, and the fact that these profiles are not simply monotonic, the experimental confidence in the determination of these kinetic parameters is illustrated by the close correspondence between the values of $K_{F/U(w)}$ and m_U derived from the equilibrium and kinetic measurements. In addition, the extrapolated value of $k_{F-I(w)}$ in D_2O matches exceedingly well with that obtained from equilibrium amide exchange experiments (see Results).

relaxation processes. The denaturant dependence of the observed relaxation rate (k_{obs}; H_2O, pH 4.5) is plotted in Figure 3. This rate profile exhibits a distinct "kink" in the folding limb, demonstrating that, in strong folding conditions, folding of CD2 proceeds via a rapidly formed intermediate species (I). Hence, the mechanism of folding of CD2 is most simply described by eq 7

$$U \underset{}{\overset{K_{I/U}}{\rightleftharpoons}} I \underset{k_{F-I}}{\overset{k_{I-F}}{\rightleftharpoons}} F \qquad (7)$$

where k_{I-F} and k_{F-I} describe rate constants for the forward and reverse processes, respectively, associated with the rate limiting I to F transition and $K_{I/U}$ the equilibrium constant associated with the rapid I to U transition. The rate profile in Figure 3 has been fitted to eq 3, allowing deduction of six physical parameters: $k_{I-F(w)}$, $k_{F-I(w)}$, $K_{I/U(w)}$, m_U, m_t, and m_I (see Table 1). The first three parameters represent rate and equilibrium constants in water, and the last three are a measure of the degree of solvation of hydrocarbon in the unfolded molecule (U), the I-F transition state (*t*), and the rapidly formed intermediate (I), respectively, all relative to the folded state (Parker *et al*., 1995). These *m* values thus provide a qualitative measure of the degree of solvent exclusion or compactness in each identifiable state in the folding reaction. Consequently, they can be used to define the position of states on a reaction coordinate for folding and unfolding, against which the free energy of a given state can be plotted (Matouschek & Fersht, 1993; Parker *et al*., 1995).

Experimental Considerations for Measuring Isotope Effects on Folding Reactions

Two hydrogen isotope effects on the energetics of protein folding reactions may be measured; a solvent-related effect and a backbone amide effect. The most rigorous way of separating these influences is to measure the kinetics of folding in four conditions: (1) protonated protein in H_2O, (2) deuterated protein in H_2O, (3) protonated protein in D_2O, and (4) deuterated protein in D_2O. This allows the isotope effects associated with the energetics of folding to be dissected into solvent−solvent, solvent−backbone, and backbone−backbone contributions (see Discussion). As the backbone will exchange over time in the mixed systems, where the protein and solvent isotopes differ, then free energy changes associated with folding and unfolding in these conditions are best done by transient kinetic methods. These measurements must be performed at a pH where the relaxation rate for folding/unfolding, at any concentration of GuHCl, is appreciably faster than any of the intrinsic exchange rates for the backbone amides.

The slowest relaxation rate for the folding reaction of CD2 at pH 4.5 and a temperature of 25 °C is 0.06 s^{-1} (denaturant activity = ∼1.7 M; see Figure 3). Using the peptide hydrogen exchange measurements of Bai *et al*. (1993), we estimate that, under these conditions, 93% of the backbone amide protons in CD2 have intrinsic exchange rates which are lower by an order of magnitude or more, so will remain in their original isotopic state. The remaining 7% have an average intrinsic exchange rate that is 6 times slower than the measured relaxations, but even these fast amides will be less than 20% exchanged during the longest measurement times. Hence, to all intents and purposes, the folding/unfolding reactions of CD2 at pH 4.5 and a temperature of 25 °C satisfy this experimental criterion. Importantly for this study, it has been shown that base-catalyzed, intrinsic exchange rate constants are not affected by solvent-related isotope effects and that such rates are essentially identical for protonated and deuterated amide groups (Connelly *et al*., 1993).

For comparing solvent-related isotope effects on the dynamics of protein folding, it is important to demonstrate that the observed changes are not a result of possible differences in electrostatic interactions, caused by p*K* shifts occurring over the range of error involved in correcting for the D^+ ion concentration. To correct for the glass electrode solvent isotope artefact, we use the relationship derived by Glascoe and Long (1960): $pD_{corr} = pD_m + 0.4$ (where pD_{corr} and pD_m are the corrected and measured D^+ ion concentrations, respectively). Rate profiles for protonated CD2 in H_2O at pH 4.0 and 5.0 are compared in Figure 3 and are seen to be directly superimposable. Thus, any possible differences measured in the dynamics of folding of CD2 in D_2O *versus* H_2O are not due to differences in side-chain ionization arising from errors in measuring the pD/pH of the solution or in isotope-related alterations of p*K*. Also worthy of note is the

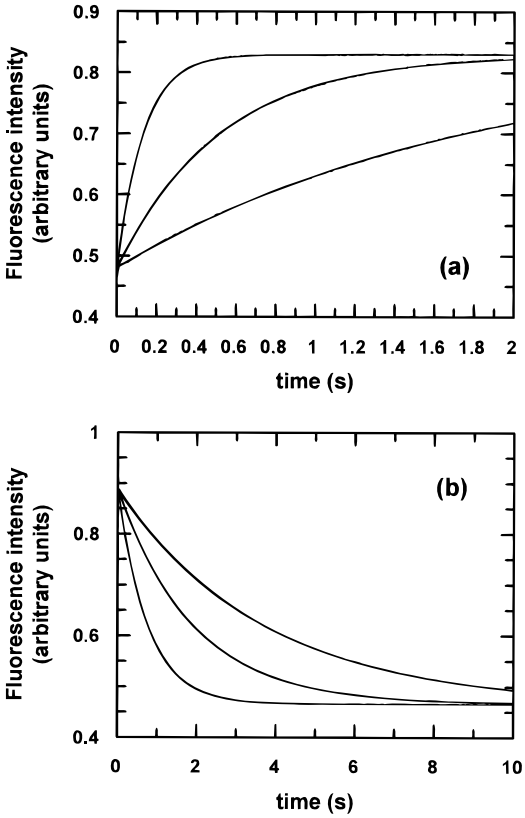

FIGURE 2: Folding and unfolding kinetics. (a) Three representative kinetic traces for the folding of protonated CD2 in H_2O (pH 4.5; $T = 25 \pm 0.1$ °C) are shown, following fluorescence intensity as a function of time. The final GuHCl concentrations are, in order from top to bottom, 0.18, 0.64 and 0.95 M and the calculated first-order rate constants (see Analytical Procedures) are 7.7, 1.9, and 0.56 s^{-1}, respectively. (b) Three representative kinetic traces for the unfolding of protonated CD2 in H_2O (pH 4.5; $T = 25 \pm 0.1$ °C). The final GuHCl concentrations are, in order from top to bottom, 3.64, 4.18, and 4.91 M, and the calculated first-order rate constants (see Analytical Procedures) are 0.77, 0.53, and 1.3 s^{-1}, respectively. Fitted curves are shown as continuous lines. Presented traces are averaged from five acquisitions. The average error in calculated rate constants does not exceed 5%. No dead time phase can be detected in the fluorescence stopped-flow measurements of the folding rates, in conditions where the intermediate is populated. The fluorescence signal change therefore represents the full signal change between the fully unfolded molecule and the folded state. Plotting the amplitudes of both the folding and unfolding transients as a function of denaturant activity produces an unfolding curve which matches exceedingly well that obtained by equilibrium measurements (data not shown).

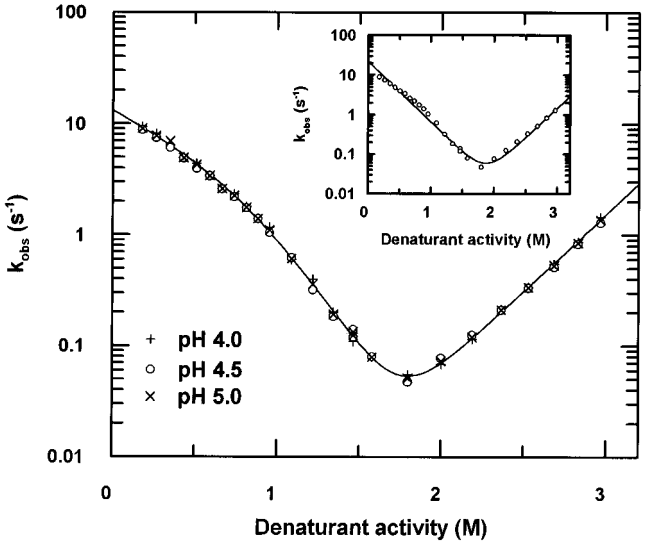

FIGURE 3: Effect of pH on folding/unfolding kinetics. The variation of observed relaxation rate (k_{obs}) for folding/unfolding as a function of denaturant activity (see Analytical Procedures and Results) is shown for protonated CD2 in H_2O, $T = 25 \pm 0.1$ °C, at pH 4.0, 4.5, and 5.0. The fact that these rate profiles are superimposable demonstrates that the effect of D_2O on the folding energetics of CD2 (see Figure 7) is not attributable to possible changes in ionization, over the range of error expected in calculating the D^+ ion concentration (±0.4 pH units, maximally; see Results). The data for pH 4.5 has been fitted to eq 3 to yield values for $k_{I-F(w)}$, $k_{F-I(w)}$, $K_{I/U(w)}$, m_I, m_t, and m_U (see Results for explanation of parameters). The fit to the data is shown as a continuous curve, and calculated values are given in Table 1. The deviation from linearity in the folding limb of these rate profiles is not due to possible temperature changes incurred from heat of dilution effects. The temperature change measured upon dilution of one part of 2 M GuHCl into 10 parts of water—the largest GuHCl dilution involved in the measurement of the folding rates—is within the experimental temperature fluctuation, estimated to be no more than ±0.1 °C (see Experimental Procedures). The data have also been analyzed in terms of a two-state mechanism (see insert; the fit is shown as a continuous curve). This yields values for $K_{F/U(w)}$ ($=k_{U-F(w)}/k_{F-U(w)}$) and m_U of $(4.68 \pm 4.41) \times 10^5$ and -6.99 ± 0.22 M^{-1}, respectively. As well as the relatively large fitting uncertainties, the data in Table 1 demonstrate the relatively poor correlation between these values and those determined from the equilibrium measurements. When analyzed in terms of a three-state mechanism, the correlation between these values is very good (see Table 1).

extremely close similarity of dielectric constant for H_2O and D_2O [78.54 and 78.25, respectively, at 25 °C; taken from Weast (1989)] showing that the solvent will have a negligible influence on charge−charge interactions

It is well established that there is a nonlinear relationship between denaturant concentration and both the free energy change of protein unfolding (Johnson & Fersht, 1995) and the solvation free energy change of protein hydrocarbon moieties (Tanford, 1970; Pace, 1975; Staniforth *et al.*, 1993). So, for the equilibrium and kinetic analyses in H_2O, GuHCl concentration ([GuHCl]) is converted to molar denaturant activity (D), according to eq 1. Where high denaturant concentrations are required to unfold a protein, this linearised scale allows a more reliable extrapolation of data to a condition where denaturant is absent. This is particularly important for the evaluation of unfolding rates and equilibrium constants in water and for determining proper *m* values.

Reassuringly, a direct calorimetric evaluation of the dependence of the free energy change of protein unfolding on denaturant concentration, performed by Johnson and Fersht (1995), provides a molar denaturation scale in very close agreement to that derived from solubility data (Parker *et al.*, 1995). This discussion prompts the question of how the free energy change associated with protein folding varies as a function of denaturant concentration in a deuterated solvent.

The dependence of the free energy change of solvation of *N*-acetyltryptophanamide (NATA) on GuHCl concentration, in H_2O and D_2O, is shown in Figure 4. This compound was chosen because its $C_{0.5}$ value (a measure of the degree of nonlinearity between concentration and activity) is close to the average for all amino acid residues, thus its behavior is representative, and its concentration can be accurately measured by absorbance. The data have been fitted to the empirical relationship given by eq 5, to yield values of $\Delta G_{s,max}$ (the maximum change in solvation free energy at an infinite concentration of denaturant) and $C_{0.5}$ (the concentration of denaturant required to achieve half this maximal

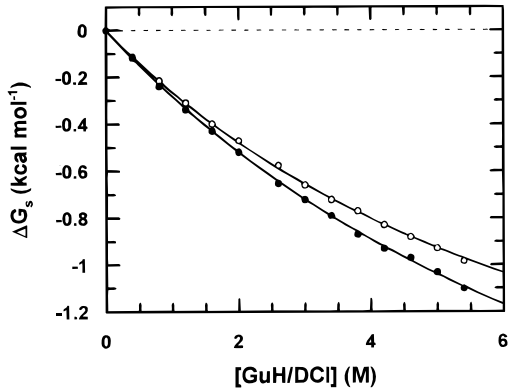

FIGURE 4: Hydrocarbon solubility in H_2O and D_2O. The free energy change of solvation of N-acetyltryptophanamide (NATA) as a function of denaturant concentration at 25 ± 0.1 °C (see Experimental Procedures and eq 4): open circles, H_2O with GuHCl; closed circles, D_2O with deuterated GuHCl (GuDCl). The data have been fitted to eq 5 to yield values of $\Delta G_{s,max}$ and $C_{0.5}$, which describe the maximum free energy change of solvation, at an infinite denaturant concentration, and the denaturant concentration required to reach half $\Delta G_{s,max}$, respectively. For H_2O, $\Delta G_{s,max} = -2.45 \pm 0.11$ kcal mol^{-1} and $C_{0.5} = 8.24 \pm 0.55$ M. For D_2O, $\Delta G_{s,max} = -3.12 \pm 0.23$ kcal mol^{-1} and $C_{0.5} = 10.0 \pm 0.10$ M. The fits to the data are shown as continuous curves.

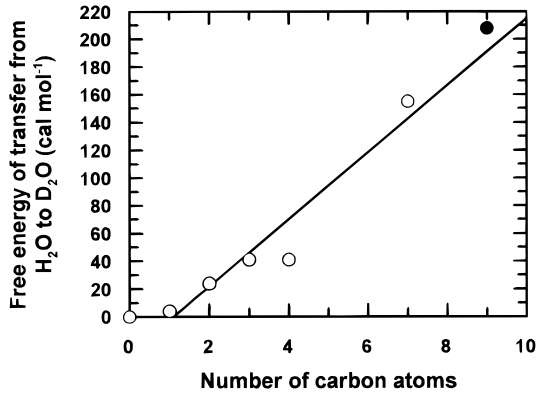

FIGURE 5: Solubility of the nonpolar amino acids in H_2O and D_2O. Here, the free energy of transfer of the nonpolar amino acids from H_2O to D_2O at 25 °C have been plotted against the number of carbon atoms [calculated relative to glycine; see Kresheck *et al*. (1965)]. Open circles, data taken from Kresheck *et al*. (1965); closed circle, difference free energy of transfer calculated for NATA between H_2O and D_2O. These data demonstrate a strong correlation (coefficient = 0.96) between the free energy of transfer from H_2O to D_2O and the number of carbon atoms for the nonpolar amino acids. The slope of the straight line fit gives a value of 24 ± 3 cal mol^{-1} per carbon atom.

change in solvation free energy). The calculated values of $\Delta G_{s,max}$ and $C_{0.5}$ for NATA, in H_2O and D_2O, are given in the legend to Figure 4. The values calculated in H_2O agree closely with those calculated from the solubility data of Tanford (1970) for the side chain of tryptophan (Parker *et al*., 1995). NATA is less soluble in D_2O than in H_2O by 0.67 ± 0.34 kcal mol^{-1}. The data of Kresheck *et al*. (1965) suggest a strong correlation between the free energy of transfer, from H_2O to D_2O, and the number of carbon atoms for the nonpolar amino acids (see Figure 5). As there is also a strong correlation between $\Delta G_{s,max}$ (for transfer from water to GuHCl solution) and the number of carbon atoms for both polar and nonpolar amino acid side chains in H_2O (Parker *et al*., 1995, 1996; Staniforth *et al*., 1993; see also Supporting Information), it is to be expected that $\Delta G_{s,max}$ in D_2O will also depend on the number of carbon atoms.

The solubility data for NATA also show that the value of $C_{0.5}$ (a measure of the molar ability of denaturant to increase the solvation of hydrocarbon in water) is increased in D_2O (see Figure 4) from 8.04 to 10.0 M. This small shift is accounted for in the denaturant-dependent data shown in Figures 1 and 7. Although this makes little difference to the relationship between denaturant activity and concentration, it is important to demonstrate that the measured differences in rate and equilibrium parameters in these different solvents (see below) are outside the experimental uncertainty involved in the determination of $C_{0.5}$. Two points are worthy of note in this regard. Firstly, the use of a denaturant activity scale provides a value for $k_{F-I(w)}$ that is in very close agreement to the observed rate of exchange for amide protons in native conditions at the EX1 limit, studied by NMR (M. J. Parker and A. R. Clarke, unpublished results). Here, for amide protons which are fully protected in F, exchange is limited by the global opening rate. If raw concentration is used, these rates differ by more than an order of magnitude (data not shown). This validates the use of the denaturant activity scale to correct for the nonlinearity between the free energy of protein folding and the concentration of denaturant. Secondly, regardless of the choice of $C_{0.5}$ value, between the limits of 7.5 and 9.1 M (see legend to Figure 7), the values derived for $k_{F-I(w)}$ in H_2O and D_2O still differ by an order of magnitude. In fact, the measured differences in rate and equilibrium parameters in these different solvents is outside the experimental uncertainty involved in the determination of $C_{0.5}$ in this range (data not shown). The choice of value for $C_{0.5}$ in this range does not alter the qualitative conclusions reported in this study (see below).

As D_2O has a viscosity relative to H_2O of ~1.2 (Kestin *et al*., 1985), it is important to establish whether this increased viscosity retards the observed rate of folding. To estimate the effect of viscosity on the folding rate of CD2 in H_2O, we measured the rates of folding in 5, 10, and 15% (v/v) glycerol. The dependence of the rate of folding on relative viscosity in this range is plotted in Figure 6. As can be seen, the effect of solvent viscosity on the measured folding rate is small and the estimated retardation in rate in D_2O owing to its higher viscosity is negligible. It is important to note, however, that the retardation in rate we see due to viscosity may be masked to some extent by an acceleration in folding rate caused by the stabilizing effect of glycerol (see legend to Figure 6). As a consequence, the acceleration in folding rate observed in the presence of D_2O may be slightly underestimated.

Isotope Effects on the Kinetics of Folding of CD2

The observed folding/unfolding rates for protonated CD2 in H_2O and D_2O and deuterated CD2 in H_2O and D_2O are plotted against denaturant activity in Figure 7a and 7b, respectively. The values of $k_{I-F(w)}$, $k_{F-I(w)}$, $K_{I/U(w)}$, $K_{F/U(w)}$, m_t, m_I, and m_U calculated from these rate profiles are given in Table 1 and have been used to construct the free energy profiles (free energy of a given state *versus* its *m* value, both relative to U) shown in Figure 8a.

The results demonstrate that the energetics of folding of CD2 are influenced only by solvent-related isotope effects,

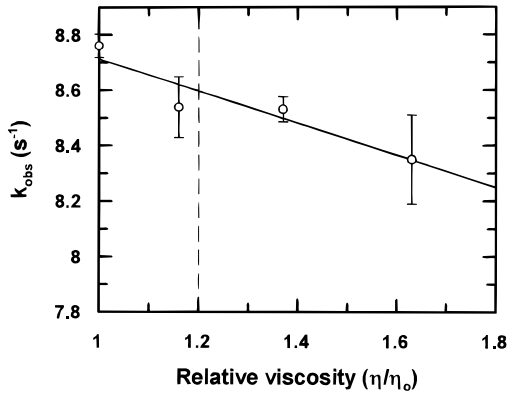

FIGURE 6: Dependence of the rate of folding on solvent viscosity. Shown here is the viscosity dependence of the folding rate of CD2 in H_2O (pH 4.5; $T = 25 \pm 0.1$ °C). The folding rate of CD2 was measured in 0, 5, 10, and 15% (v/v) glycerol solutions (see Experimental Procedures), which have relative viscosities of 1.00, 1.16, 1.37, and 1.63, respectively [taken from Weast (1989)]. The relative viscosity of D_2O is ~1.2 (Kestin *et al*., 1985) and is marked here by a dashed line. The data has been fitted to a straight line, so that the expected retardation of the folding rate in D_2O, due to viscosity, can be estimated. Equilibrium unfolding measurements of protonated CD2 in H_2O reveal, however, that the addition of 5% glycerol increases the stability of the folded state by ~0.35 kcal mol^{-1}, relative to the unfolded state (data not shown). Consequently, the retardation in rate caused by increased viscosity may be underestimated to some extent, as the stabilizing effect of glycerol might actually accelerate the folding process.

increasing the stabilities of the intermediate state (I), the I-F transition state (t), and the folded state (F), by an average of 0.53, 0.68, and 1.26 kcal mol^{-1}, respectively, all relative to the unfolded state (U). The kinetics of folding/unfolding of protonated and deuterated CD2 are identical to each other when measured in the same solvent. In other words, there are no measurable isotope effects associated with the exchange of backbone−backbone (amide:carbonyl) hydrogen bonds for backbone−solvent (amide:water) bonds (see Discussion).

For the bulk solvent isotope effect, the difference free energies ($\Delta\Delta G$) for each state are plotted against their *m* values (both relative to U) in Figure 8b. The correlation between $\Delta\Delta G$ and m demonstrates that the bulk solvent isotope effect on the stability of each state, relative to U, depends on the fractional degree to which hydrocarbon is desolvated in these states.

DISCUSSION

Comparing the relaxation kinetics of folding and unfolding of a protonated and a deuterated protein in H_2O and in D_2O allows dissection of the isotope effects associated with the free energies of solvent−solvent (H_2O:HOH), solvent−backbone (H_2O:HN and C═O:HOH), and backbone−backbone (C═O:HN) hydrogen bonding interactions (see Supporting Information for an inventory of hydrogen bonds made and broken during unfolding). The results of this study show that, for all transitions, the free energy changes of folding/unfolding for protonated and deuterated CD2 in H_2O are the same. Similarly, the folding/unfolding kinetics of protonated and deuterated CD2 in D_2O are indistinguishable from each other, i.e., the isotope effect on the C═O:HN bond is the same as that on the H_2O:HN bond. A similar observation has also been made by Itzhaki and Evans (1996), who found that the rate of folding of lysozyme in H_2O is not sensitive to isotopic substitution of the amide backbone. However, it is important to stress that the absence of an amide-based isotope effect provides no information on the net contribution of backbone hydrogen bonding to the stability of the native state, i.e., the results cast no light on the relative strength of C═O:HN and H_2O:HN bonds.

The appreciable isotope effect arising from the protein folding in D_2O rather than H_2O is more physically illuminating. If it is assumed that there is no secondary isotope effect resulting from the substitution of non-bonding hydrogens (i.e., H_2O:HN has the same strength as D_2O:HN) then one component of the measured effect results from the energy difference in isotopically substituting those hydrogen bonds made between water molecules and acceptors on the protein. The new acceptors which become exposed on unfolding are predominantly backbone carbonyls (e.g., C═O:HOH). Since, from the analysis above, it is known that the energy difference between the C═O:HN and C═O:DN hydrogen bonds is the same as that between the H_2O:HN and H_2O:DN hydrogen bonds, it appears reasonable to assume that H/D substitutions have similar energetic effects in these uncharged bonding systems, irrespective of the nature of the donor and acceptor groups. This leads to the expectation that the free energy difference between the H_2O:HOH bond and the D_2O:DOD would be the same as that between C═O:HOH and C═O:DOD. If this is the case, then the isotope effect must result from a process which does not involve the exchange of hydrogen bonds between solvent and backbone groups. The most likely source of this effect is the difference in the free energy of solvation of those hydrocarbon groups which become exposed to solvent upon unfolding. This is evidenced by the unfavorable free energy of transfer of nonpolar amino acid groups from H_2O to D_2O and the correlation between this free energy change of transfer and the number of carbon atoms (see Figure 5).

As described in Results, relative to the unfolded state, the stabilities of the rapidly formed intermediate (I), the rate-limiting transition state (t), and the folded state (F) are increased in D_2O, by an amount that is proportional to their *m* values (Figure 8b). Along with others (Alonso & Dill, 1991; Kuwajima *et al*., 1989; Matouschek & Fersht, 1993; Shortle *et al*., 1988; Tanford, 1970), we interpret the *m* value as a measure of the increase in the exposure of protein hydrocarbon that is inaccessible to solvent in the folded state. This interpretation is confirmed by at least two experimental observations. Firstly, there is a close link between the *m* value for a protein unfolding transition and the associated change in heat capacity (Shortle *et al*., 1988; Myers *et al*., 1995); the latter being taken as a measure of the extra heat involved in melting ordered water molecules at the nonpolar solute−water interface (Frank & Evans, 1945; Gill *et al*., 1985; Muller, 1990; Nemethy & Scheraga, 1962; Spolar *et al*., 1989). Secondly, there is a tight correlation between the number of nonpolar residues exposed in an unfolding step, the *m* value of the transition and the empirically determined solvation energy for that collection of amino acids which are buried in the folded state (Staniforth *et al*., 1993; see also Supporting Information).

Both experimental (Benjamin & Benson, 1962) and theoretical (Scheiner & Cuma, 1996) studies have demonstrated that deuterium bonds are stronger than hydrogen bonds in water, by 0.1−0.2 kcal mol^{-1}. The increased strength of the deuterium bond in water is attributed to the

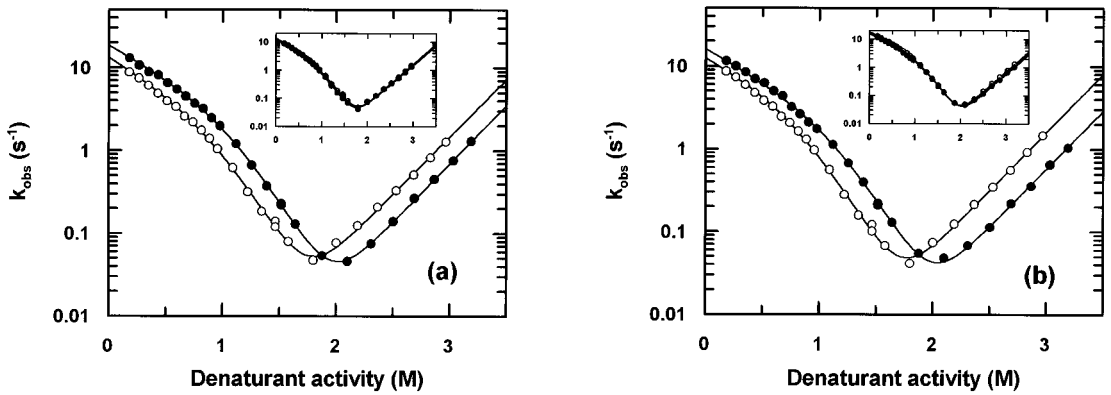

FIGURE 7: Isotope effects on the kinetics of folding/unfolding of CD2. The denaturant dependence of the observed rate of folding/unfolding (k_{obs}) for protonated CD2 (^{NH}CD2; panel a) and deuterated CD2 (NDCD2; panel b) are shown in protonated and deuterated solvents (open and closed circles, respectively). For the data collected in H_2O, [GuHCl] has been converted to denaturant activity according to eq 1, using a $C_{0.5}$ value of 7.5 M [see Parker et al. (1995) and Results]. For the data collected in D_2O, a $C_{0.5}$ value of 9.1 M was chosen, using the fractional difference in $C_{0.5}$ calculated for NATA in H_2O and D_2O [i.e., 7.5 M × (10.0/8.24); see legend to Figure 4]. All of these data have been fitted to eq 3 to yield values for $k_{I-F(w)}$, $k_{F-I(w)}$, $K_{I/U(w)}$, m_I, m_t, and m_U. Fits to the data are shown as continuous curves, and the calculated values are given in Table 1. All these data are averaged from two repeated sets of experiments. The rate profiles obtained for ^{NH}CD2 and NDCD2, in H_2O and D_2O, are highly reproducible, using both freshly prepared protein samples and denaturant solutions. In fact, for both the kinetic and equilibrium measurements, the estimated experimental uncertainties in the derived parameters are comparable to the fitting uncertainties. The insets in a and b demonstrate the superimposition of rate profiles for ^{NH}CD2 and NDCD2 in H_2O and in D_2O, respectively. The *m* values, which describe the fractional difference in the solvation of hydrocarbon between states (see Discussion), are the same in H_2O and D_2O, within experimental error (see Table 1).

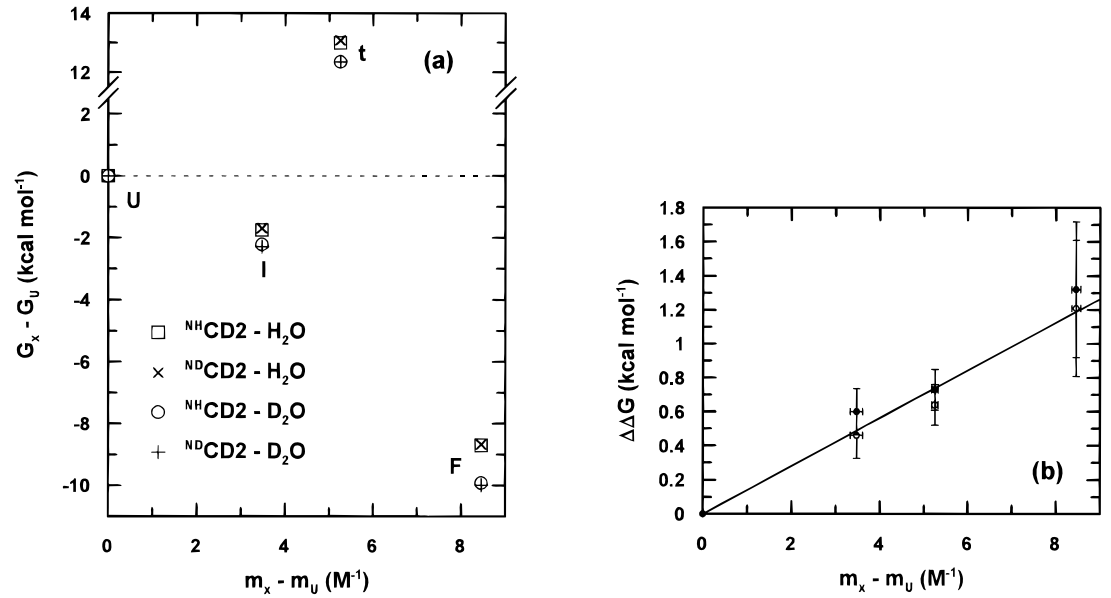

FIGURE 8: Isotope effects on the free energy "reaction coordinate" of protein folding. (a) Free energies of the intermediate (I), rate-limiting transition state (t), and folded state (F), all relative to the unfolded state (U), have been plotted against their *m* values (also relative to U), for protonated and deuterated CD2 folding in protonated and deuterated solvent. For the purposes of this plot, the rate of interconversion between F and I, for an activationless process, is arbitrarily set at 10^{12} s^{-1} (the upper rate of rotational reorganization of side chains in molecular mechanical simulations of peptides; R. B. Sessions, personal communication). As can be seen from the plot, the energetics of folding of protonated CD2 (^{NH}CD2) and deuterated CD2 (NDCD2) are identical in either solvent conditions. The only measurable isotope effect on the energetics of folding is associated with the properties of the bulk solvent. (b) Difference free energy for each state, between protonated and deuterated solvents, is plotted against its *m* value, relative to U (open circles, ^{NH}CD2; closed circles, NDCD2). These data fit a straight line with a correlation of 0.97 and demonstrate that each state is stabilized in D_2O according to its fractional degree of solvation of hydrocarbon (see Discussion). In a and b, the subscript "x" defines the U, I, t, and F states, as indicated.

higher mass of the deuteron lowering the zero-point vibrational energy of the intermolecular mode of highest frequency, associated with a bending motion of the proton donor molecule, which distorts the linearity of the hydrogen bond (Scheiner & Cuma, 1996). From this and the above discussion, it would appear that, at 25 °C, an increase in the hydrophobic interaction in protein folding is commensurate with an increased enthalpic water−water affinity. In other words, the energetic favorability of burying nonpolar amino acid side chains upon protein folding is modulated, at least in part, by the cohesive properties of the bulk solvent. As discussed by Dill (1990), this operational description of the hydrophobic interaction is not subject to the Hildebrand objection (Hildebrand, 1968, 1979), i.e., "that hydrophobicity is not an enthalpic disaffinity of nonpolar solutes for water but instead is due to a water−water affinity". While it would be dangerous to conclude anything about exact contributions to the hydrophobic interaction, the data presented here do not support the theory that the free energy of hydration of nonpolar groups at 25 °C is favorable and that, consequently,

the hydrophobic effect in proteins arises only from enthalpic interactions between protein groups (Privalov & Gill, 1988; Privalov, 1989).

The results we describe also have practical implications for amide hydrogen exchange studies of protein folding mechanisms (Roder *et al*., 1988; Udgaonkar & Baldwin, 1988). Firstly, because the stabilities of states in the folding reaction are influenced by the isotopic nature of the bulk solvent, it is important to establish the behavior of the system in D_2O and in H_2O when the equilibrium position and/or rates of folding steps are used to interpret measured protection factors. Secondly, the observation that isotopic substitution of the backbone NH does not change the relative stability of states in folding mechanisms demonstrates that during H/D exchange experiments isotopic substitution will not perturb the energetics of the system.

ACKNOWLEDGMENT

We thank the B.B.S.R.C. (U.K.) for project funding and the Wellcome Trust for an equipment grant. A.R.C. is a Lister Institute research fellow.

SUPPORTING INFORMATION AVAILABLE

Data are provided which show the strong correlation between the maximum free energy of solvation, from water to GuHCl, and the number of carbon atoms, for both polar and nonpolar amino acid side chains; also an inventory of hydrogen bonds made and broken during folding and unfolding, along with the energetic components which make up the measured isotope effects (4 pages). Ordering information is given on any current masthead page.

REFERENCES

Alonso, D. O. V., & Dill, K. A. (1991) *Biochemistry 30*, 5974−5985.
Bai, Y., Milne, J. S., Mayne, L., & Englander, S. W. (1993) *Proteins: Struct., Funct., Genet. 17*, 75−86.
Benjamin, L., & Benson, G. C. (1962) *J. Phys. Chem. 67*, 858−861.
Connelly, G. P., Bai, Y., Jeng, M. F., & Englander, S. W. (1993) *Proteins: Struct., Funct., Genet. 17*, 87−92.
Creighton, T. E. (1991) *Curr. Opin. Struct. Biol. 1*, 5−16.
Creswell, C. J., & Allred, A. L. (1962) *J. Am. Chem. Soc. 84*, 3966−3967.
Dill, K. A. (1990) *Biochemistry 29*, 7133−7155.
Driscoll, P. C., Cyster, J. G., Campbell, I. D., & Williams, A. F. (1991) *Nature 353*, 762−765.
Frank, H. S., & Evans, M. W. (1945) *J. Chem. Phys. 13*, 507−515.
Gill, S. J., Dec, S. F., Olofsson, G., & Wadso, I. (1985) *J. Phys. Chem. 89*, 3758−3765.
Glascoe, P. F., & Long, F. A. (1960) *J. Phys. Chem. 64*, 188−193.
Hermans, J., Jr., & Scheraga, H. A. (1959) *Biochim. Biophys. Acta. 36*, 534−535.
Hildebrand, J. H. (1968) *J. Phys. Chem. 72*, 1841−1842.
Hildebrand, J. H. (1979) *Proc. Natl. Acad. Sci. U.S.A. 76*, 194.
Honig, B., & Yang, A. S. (1995) *Adv. Protein Chem. 46*, 27−58.
Itzhaki, L. S., & Evans, P. A. (1996) *Protein Sci. 5*, 140−146.
Johnson, C. M., & Fersht, A. R. (1995) *Biochemistry 34*, 6975−6804.
Kestin, J., Imaishi, N. Nott, S. H., Nieuwoudt, J. C., & Sengers, J. V. (1985) *Physica 134A*, 38−58.
Kresheck, G. C., Schneider, H., & Scheraga, H. A. (1965) *J. Phys. Chem. 69*, 3132−3144.
Kuwajima, K., Mitani, M., & Sugai, S. (1989) *J. Mol. Biol. 206*, 547−561.
Makhatadze, G. I., & Privalov, P. L. (1994) *Biophys. Chem. 51*, 291−309.
Makhatadze, G. I., Clore, G. M., & Gronenborn, A. M. (1995) *Nat. Struct. Biol. 2*, 852−855.
Matouschek, A., & Fersht, A. R. (1993) *Proc. Natl. Acad. Sci. U.S.A. 90*, 7814−7818.
Muller, N. (1990) *Acc. Chem. Res. 23*, 23−28.
Murray, A. J., Lewis, S. J., Barclay, A. N., & Brady (1995) *Proc. Natl. Acad. Sci. U.S.A. 92*, 7337−7341.
Myers, J. K., Pace, C. N., & Scholtz, J. M. (1995) *Protein Sci. 4*, 2138−2148.
Nemethy, G., & Scheraga, H. A. (1962) *J. Phys. Chem. 36*, 3401−3408.
Pace, C. N. (1975) *CRC Crit. Rev. Biochem. 3*, 1−43.
Pace, C. N., Shirley, B. A., McNutt, M., & Gajiwala, K. (1996) *FASEB J. 10*, 75−83.
Parker, M. J., Spencer, J., & Clarke, A. R. (1995) *J. Mol. Biol. 253*, 771−786.
Parker, M. J., Sessions, R. B., Badcoe, I. G., & Clarke, A. R. (1996) *Folding Des. 1*, 145−156.
Privalov, P. L. (1989) *Annu. Rev. Biophys. Chem. 18*, 47−69.
Privalov, P. L., & Gill, S. J. (1988) *Adv. Protein Chem. 39*, 191−234.
Roder, H., Elöve, G. A., & Englander, S. W. (1988) *Nature 335*, 700−704.
Sambrook, J., Fritsch, E. F., & Maniatis, T. (1989) in *Molecular Cloning: A Laboratory Manual*, 2nd ed., Cold Spring Harbor Laboratory Press, Plainview, NY.
Scheiner, S., & Cuma, M. (1996) *J. Am. Chem. Soc. 118*, 1511−1521.
Shortle, D., Meeker, A. K., & Freire, E. (1988) *Biochemistry 27*, 4761−4768.
Spolar, R. S., Livingstone, J. R., & Record, M. T., Jr. (1992) *Biochemistry 31*, 3947−3955.
Staniforth, R. A., Burston, S. G., Smith, C. J., Jackson, G. S., Badcoe, I. G., Atkinson, T., Holbrook, J. J., & Clarke, A. R. (1993) *Biochemistry 32*, 3842−3851.
Tanford, C. (1970) *Adv. Protein Chem. 24*, 1−95.
Udgaonkar, J. B., & Baldwin, R. L. (1988) *Nature 335*, 694−699.
Weast, R. C. (1989) *Handbook of Chemistry and Physics*, 70th ed., CRC Press, Inc., Boca Raton, FL.

BI9629283